

Positron binding to alkali-metal hydrides: The role of molecular vibrations

Franco A. Gianturco* and Jan Franz†

Department of Chemistry and INFM, University of Rome La Sapienza, Piazzale A. Moro 5, 00185 Rome, Italy

Robert J. Buenker and Heinz-Peter Liebermann

Fachbereich C-Mathematik und Naturwissenschaften, Bergische Universitaet Wuppertal, Gausstrasse 20, D-42119 Wuppertal, Germany

Lukáš Pichl‡ and Jan-Michael Rost

Max Planck Institute for the Physics of Complex Systems, Noethnitzer St. 38, D-01187 Dresden, Germany

Masanori Tachikawa

Graduate School of Science, Yokohama-city University, Seto 22-2, Kanazawa-ku, Yokohama 236-0027, Japan

Mineo Kimura

Graduate School of Sciences, Kyushu University, Fukuoka 812-8581, Japan

(Received 6 October 2005; published 6 February 2006)

The bound vibrational levels for $J=0$ have been computed for the series of alkali-metal hydride molecules from LiH to RbH, including NaH and KH. For all four molecules the corresponding potential-energy curves have been obtained for each isolated species and for its positron-bound complex (e^+XH). It is found that the calculated positron affinity values strongly depend on the molecular vibrational state for which they are obtained and invariably increase as the molecular vibrational energy content increases. The consequences of our findings on the likelihood of possibly detecting such weakly bound species are briefly discussed.

DOI: [10.1103/PhysRevA.73.022705](https://doi.org/10.1103/PhysRevA.73.022705)

PACS number(s): 34.10.+x, 36.10.Dr, 82.30.Gg

I. INTRODUCTION

Because of the special properties of the antiparticle of the electron, i.e., the positron, its study at the molecular level in molecular environments has been slower to come by, both at the level of experimental reliability and of theoretical and/or computational feasibility (for a recent review see [1]). The corresponding comparative analysis of the behavior of the two leptons in molecular gases has also recently provided a great deal of insight into what one can expect to happen when a slow beam of positrons interacts with molecules in the gas phase [2]. We know, in fact, that a slow electron can interact with the molecular field and could be trapped by it, thereby forming an initial resonant state that can decay into a possible bound anionic state as one of the various channels opens to its evolution [3]. It can, therefore, be speculated that the positron may also undergo a similar process and may, therefore, be able to bind to a molecule and form a stable positive molecular ion before decay either by annihilation or by molecular fragmentation [4]. On the other hand, there is still no direct experimental confirmation that a positron could be bound to a molecular partner. One of the crucial differ-

ences when contrasting atoms with molecules as possible sources of cationic species by positron impact is obviously given by the presence of the nuclear motions in the latter partner as opposed to the former. It is also well known, however, that positrons find a rather hostile environment in molecular systems, where the strongly repulsive nuclear regions (albeit screened by the bound electrons) are not entered (classically speaking) by the lepton which chiefly interacts with the outer rim of the molecular charge distribution [5], and therefore might form rather diffuse bound states through polarization-correlation forces. This is one of the reasons why both experiments and theory [6] have found that molecules are not efficiently excited vibrationally during the impact by low-energy positrons. However, because the long-range (LR) interaction region often allows for the presence of the reactive channel of Positronium (Ps) formation, then it is reasonable to expect that upon positron attachment to a molecule, or upon threshold resonance processes at vanishing collision energies [7], the molecular geometry could become distorted and therefore affect the balance involved in determining positron affinity (PA) values for gaseous molecules.

The present study intends to show, in fact, how the vibrational structures of simple diatomics such as the alkali-metal hydrides are modified upon positron attachment and therefore exhibit marked changes in the values of their PAs as a function of the molecular vibrational content.

Diffusion Monte Carlo (DMC) computational studies on annihilation rates of positrons with LiH molecules have been carried out before [8,9] for different nuclear geometries and will be compared below with the present findings.

*Corresponding author; Fax: +39-06-499913305; Email address: fa.gianturco@caspur.it

†Present address: Department of Physics and Astronomy, University College London, London WC1E 6BT, United Kingdom.

‡On leave from International Christian University, Osawa 3-10-2, Mitaka, Tokyo 181-8585, Japan.

TABLE I. Computed minimum energy geometry from the present PECs of the alkali-metal hydrides and of their complexes with a positron. All values in bohr.

Molecule	R_{eq} (MH)	$R_{eq}(e^+MH)$
LiH	3.014	3.324
NaH	3.566	4.095
KH	4.246	5.061
RbH	4.418	5.478

The following section summarizes our calculations of the vibrational levels while Sec. III reports our results for the calculated PA values and other positron complex characteristics. Finally, Sec. IV draws our current conclusions.

II. MOLECULAR VIBRATIONAL STRUCTURES

The calculations of the total, Born-Oppenheimer (BO) electronic energies for the series of molecules we are analyzing in the present work (LiH, NaH, KH, RbH) have been discussed in great detail in a recent paper [10] and therefore we will not repeat here their description. Suffice to say that all calculations were at the post-Hartree-Fock level and were carried out using a multireference single- and double-

TABLE II. Vibrational energy levels for LiH and e^+LiH . The relative spacing $\Delta E_\nu = E_\nu - E_{\nu-1}$ is also given. The dissociation energy values D_0 are also shown. All values in eV.

ν	$E_\nu(\text{LiH})$	$\Delta E_\nu(\text{LiH})$	$E_\nu(e^+\text{LiH})$	$\Delta E_\nu(e^+\text{LiH})$
0	0.087	0.087	0.061	0.061
1	0.256	0.169	0.182	0.121
2	0.419	0.163	0.298	0.116
3	0.577	0.158	0.398	0.100
4	0.729	0.152	0.493	0.095
5	0.876	0.147	0.580	0.087
6	1.019	0.143	0.660	0.080
7	1.156	0.137	0.734	0.074
8	1.288	0.132	0.801	0.067
9	1.415	0.127	0.862	0.061
10	1.537	0.122	0.917	0.055
11	1.654	0.107	0.965	0.048
12	1.766	0.112	1.008	0.043
13	1.873	0.107	1.044	0.036
14	1.975	0.102	1.075	0.031
15	2.071	0.096	1.099	0.024
16	2.160	0.089	1.117	0.018
17	2.243	0.083	1.130	0.013
18	2.319	0.076		
19	2.386	0.067		
20	2.443	0.057		
D_0	2.534		1.133	

TABLE III. Vibrational energy levels for NaH and e^+NaH . The relative spacing $\Delta E_\nu = E_\nu - E_{\nu-1}$ is also given. The dissociation energy values D_0 are also shown. All values in eV.

ν	$E_\nu(\text{NaH})$	$\Delta E_\nu(\text{NaH})$	$E_\nu(e^+\text{NaH})$	$\Delta E_\nu(e^+\text{NaH})$
0	0.072	0.072	0.042	0.042
1	0.211	0.139	0.121	0.079
2	0.347	0.136	0.195	0.074
3	0.478	0.131	0.262	0.067
4	0.605	0.127	0.325	0.063
5	0.727	0.122	0.381	0.056
6	0.845	0.118	0.433	0.052
7	0.959	0.114	0.481	0.048
8	1.068	0.109	0.524	0.043
9	1.173	0.105	0.562	0.038
10	1.274	0.101	0.597	0.035
11	1.369	0.095	0.629	0.029
12	1.460	0.091	0.648	0.022
13	1.546	0.086	0.664	0.016
14	1.627	0.081	0.675	0.011
15	1.700	0.073		
16	1.767	0.067		
17	1.826	0.059		
18	1.876	0.050		
19	1.915	0.039		
20	1.942	0.027		
D_0	1.955		0.678	

excitation configuration interaction (MRD-CI) approach that employs a new computational code which makes use of the Table-Direct-CI method [11,12] for the construction of the required Hamiltonian matrix elements and electron and/or positron bound wave functions. The range of nuclear geometries which were considered varied from $R_{min}=1.50$ to $R_{max}=12.0$ bohr for the LiH molecule and from $R_{min}=1.50$ to $R_{max}=14.0$ bohr for the e^+LiH complex. Likewise, the radial ranges for NaH and e^+NaH went from $R_{min}=2.00$ to R_{max} values of 12.00 and 15.00 bohr, respectively. The KH and e^+KH molecules were also calculated from $R_{min}=2.00$ and 2.50 to the R_{max} values of 20.00 and 15.00 bohr, respectively. Finally, the calculations for the RbH and e^+RbH molecules ranged from $R_{min}=2.50$ and 3.00 bohr to the R_{max} values of 25.00 and 15.00 bohr. The corresponding values of the potential minima are given by Table I, where the quality of the employed basis set is that defined earlier on as the ‘‘FCI core’’ choice [8]. The results for LiH and e^+LiH are very close to those given by Ref. [9]. Here again we do not wish to discuss the quality of the selected basis set for generating the different potential energy curves (PECs), since this discussion was already the subject of the work reported by Ref. [10], while we want to stress that the results of Table I clearly indicate a marked bond deformation upon positron attachment to all four title molecules. This deformation effect, which can be related to the ‘‘bond dilution’’ consequences of Ps formation within the molecular bound elec-

TABLE IV. Vibrational energy levels for NaH and e^+ KH. The relative spacing $\Delta E_\nu = E_\nu - E_{\nu-1}$ is also given. The dissociation energy values D_0 are also shown. All values in eV.

ν	$E_\nu(\text{KH})$	$\Delta E_\nu(\text{KH})$	$E_\nu(e^+\text{KH})$	$\Delta E_\nu(e^+\text{KH})$
0	0.061	0.061	0.030	0.030
1	0.181	0.120	0.084	0.054
2	0.297	0.116	0.134	0.050
3	0.411	0.114	0.177	0.043
4	0.522	0.111	0.216	0.039
5	0.630	0.108	0.249	0.033
6	0.735	0.105	0.277	0.028
7	0.837	0.102	0.299	0.022
8	0.936	0.099	0.315	0.016
9	1.031	0.095	0.324	0.009
10	1.123	0.092		
11	1.211	0.088		
12	1.296	0.085		
13	1.379	0.083		
14	1.459	0.080		
15	1.537	0.078		
16	1.613	0.076		
17	1.687	0.074		
18	1.759	0.072		
19	1.829	0.070		
20	1.895	0.066		
D_0	1.985		0.327	

 TABLE V. Vibrational energy levels for RbH and e^+ RbH. The relative spacing $\Delta E_\nu = E_\nu - E_{\nu-1}$ and the dissociation energy values D_0 are also shown. All values in eV.

ν	$E_\nu(\text{RbH})$	$\Delta E_\nu(\text{RbH})$	$E_\nu(e^+\text{RbH})$	$\Delta E_\nu(e^+\text{RbH})$
0	0.060	0.060	0.021	0.021
1	0.179	0.119	0.062	0.041
2	0.292	0.113	0.099	0.037
3	0.402	0.110	0.131	0.032
4	0.507	0.105	0.159	0.028
5	0.609	0.102	0.181	0.022
6	0.708	0.099	0.199	0.018
7	0.804	0.096	0.211	0.012
8	0.897	0.093	0.217	0.006
9	0.987	0.090		
10	1.074	0.087		
11	1.158	0.084		
12	1.239	0.081		
13	1.318	0.079		
14	1.394	0.076		
15	1.467	0.073		
16	1.538	0.071		
17	1.608	0.070		
18	1.675	0.067		
19	1.739	0.064		
20	1.800	0.061		
D_0	2.025		0.217	

trons, plays a significant role as one increases the vibrational content of the molecule bound to the e^+ partner, the object of the present study.

The final potential energy curves for all four systems, and for their positron-bound complexes, have been spline-fitted and employed to generate the $J=0$ vibrational bound states using the LEVEL computer code [13], over a very dense radial grid and stabilizing the final results with respect to both the radial range of the PES employed and the grid density of radial values selected in the integration.

Tables II–V report, for all four systems, the distributions of the vibrational levels and their respective energy spacings ΔE_ν . Each table shows the level spectrum for the isolated molecule and for its complex with the positron. The following considerations could be readily made.

(1) The number of bound states decreases when going from LiH to RbH, indicative of the corresponding reductions of the well depths that vary from about 20 000 cm^{-1} for LiH to about 18 000 cm^{-1} for RbH, while the reduced mass only slightly increases from Li to Rb.

(2) The complexes with one positron bound to a molecule also show marked variations in going from LiH to RbH: each complex is thought of as having the alkali-metal ion as one of the asymptotic partners, with the corresponding formation of a Ps compound bound to a hydrogen atom: $X^+ + \text{HPs}$ [10]. The corresponding well depths thus decrease from about 9 000 cm^{-1} for $e^+\text{LiH}$ to about 1 700 cm^{-1} for $e^+\text{RbH}$.

(3) The spacings between vibrational levels are also seen to depart from harmonicity for the PECs associated to the complex more quickly as the quantum number increases than in the cases where the isolated molecule is considered. This difference will be seen below to play an important role in our discussion of the PA dependence on the target vibrational quantum state. For the case of LiH and $e^+\text{LiH}$ the vibrational spacings we found are within a few percent of those obtained in Ref. [9] using DMC calculations.

To make the present analysis pictorially more transparent, we report in Fig. 1 the potential-energy curves for the four XH systems (solid lines) and below each of them the corresponding curves for the $e^+\text{XH}$ complex. The corresponding lower vibrational levels for each couplet of curves are shown at their relative locations for each system. One clearly sees there that the coupling between each set of states strongly depends on the system in the sense that the initial, $\nu=0$ state of each XH hydride overlaps in energy with a different region of vibrational states of its complex with e^+ . One consequence of this situation could be better gleaned when looking at the Franck-Condon (FC) factors between each $\text{XH}(\nu=0)$ initial state and all possible final vibrational states of the corresponding $e^+\text{XH}$ complex. These factors are reported specifically by Table VI.

It is clear that the largest probability given by the FC factors indicate the lowest vibrational level of the $e^+\text{XH}$ complex to be the most probable for LiH, while NaH shows

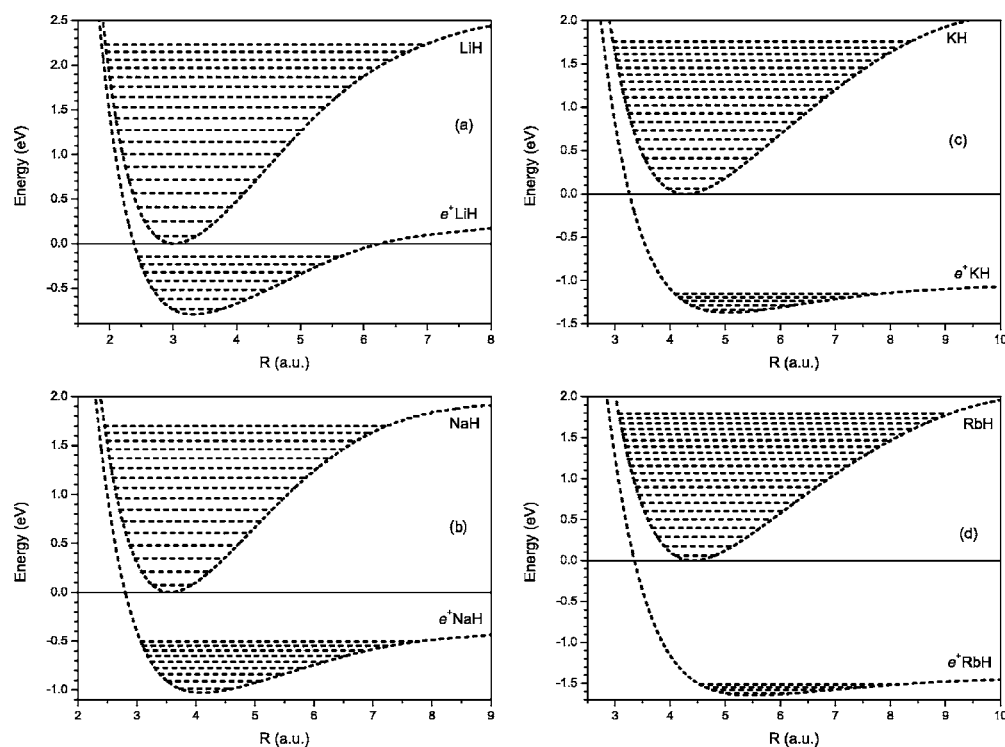


FIG. 1. Potential-energy curves for all the four alkali-metal hydrides and for their positron complexes, (a) LiH, (b) NaH, (c) KH, and (d) RbH. The energy is set to zero for the neutral species at its equilibrium geometry. The lower vibrational levels are shown for both sets of curves.

TABLE VI. Franck-Condon factors $S_{0\nu}$ for the transition from the zeroth vibrational level of the neutral to the ν th vibrational level of the positron attached to it.

Molecule	LiH ^a	KH ^a	NaH ^a	RbH ^a
Final state	$S_{0\nu}$	$S_{0\nu}$	$S_{0\nu}$	$S_{0\nu}$
0	6.2961(-1)	3.1467(-1)	1.2259(-1)	3.0407(-2)
1	2.7461(-1)	3.0428(-1)	1.9030(-1)	7.1957(-2)
2	7.1098(-2)	1.8963(-1)	1.8398(-1)	9.0141(-2)
3	1.8426(-2)	9.9120(-2)	1.4458(-1)	9.3569(-2)
4	4.6541(-3)	4.7939(-2)	1.0207(-1)	8.6057(-2)
5	1.1951(-3)	2.2625(-2)	6.8733(-2)	7.0555(-2)
6	3.0533(-4)	1.0768(-2)	4.4536(-2)	5.1125(-2)
7	7.8486(-5)	5.2268(-3)	2.7998(-2)	2.9533(-2)
8	1.9440(-5)	2.6043(-3)	1.6085(-2)	7.6744(-3)
9	4.1247(-6)	1.3325(-3)	7.8860(-3)	
10	5.7997(-7)	7.0100(-4)		
11	1.0656(-8)	3.6950(-4)		
12	4.8494(-8)	1.9496(-4)		
13	1.2980(-7)	1.0486(-4)		
14	1.5608(-7)	4.8834(-5)		
15	1.3720(-7)			
16	1.0572(-7)			
17	6.5684(-8)			

^aThe notation: $d.dd(-e)$ means: $d.dd \times 10^{-e}$.

similar values up to $\nu=2$, KH indicates to form its complex more likely in the $\nu=1$ and 2 levels, and RbH suggests that a vibrationally excited complex state is definitely more likely to occur than its ground vibrational state.

III. THE POSITRON AFFINITIES

In terms of the simplest thermochemical view, one can define the binding energy of one positron to the neutral XH partner as the PA,

$$[\text{PA}(R_{eq})] = E_{(R_{eq})}^{XH} - E_{(R_{eq})}^{e^+XH}, \quad (1)$$

where both calculations correspond to the optimized, classical nuclear geometries of the isolated alkali-metal hydride and of its complex with the positron, respectively.

On the other hand, one can also refine the above definition by further including the zero-point-energy (ZPE) corrections and by considering the involved species in their respective ground vibrational levels $\nu=0$,

$$[\text{PA}(\nu=0)] = E_{(\nu=0)}^{XH} - E_{(\nu=0)}^{e^+XH}. \quad (2)$$

By the same token, one could consider the effects of having vibrationally “hot” molecules during the complex formation by further defining a PA value explicitly dependent on the quantum vibrational state of the positronic complex, with the condition that the quantum number remains the same after positron attachment. In other words, a partially adiabatic process is considered in which the complex undergoes geometry relaxation after positron attachment but retains the same

TABLE VII. Computed PA values from the present calculations (in eV), using Eqs. (1), (2), and (4) of main text.

Molecule	$PA(R_{eq})$	$PA_{\nu=0}$	$\Delta PA/\text{meV}$	$PA_{BO}(0)$	$\Delta PA/\text{meV}$
LiH	0.794	0.820	26	0.765	-29
NaH	1.031	1.061	30	0.954	-77
KH	1.364	1.395	31	1.270	-94
RbH	1.639	1.678	39	1.486	-153

quantum number as in the neutral target molecule with which the positron was originally interacting,

$$[PA(\nu)] = E_{(\nu)}^{XH} - E_{(\nu)}^{e^+XH}. \quad (3)$$

Finally, since the positron is a light particle, it is also interesting to evaluate the positron affinity in the Born Oppenheimer framework, i.e., within the picture of an immediate positron attachment to the alkali-metal hydride molecule at a given geometry, modulated by the vibrational wave function of the initial system before the relaxation process starts to take place, i.e., define $PA_{BO}(\nu)$ as given by

$$\int_0^\infty [E_{(\nu)}^{XH}(R) - E_{(\nu)}^{e^+XH}(R)] [\Psi_\nu^{XH}(R)]^2 dR. \quad (4)$$

The above variety of slightly different definitions of the positron affinity value in the gas phase could therefore, help us in shedding more light on the molecular mechanism of the positron attachment to a given partner and on the possible role played by the vibrational energy content of the gaseous molecule. The results from the calculations in Eqs. (1), (2), and (4) with $\nu=0$ are shown in Table VII.

It is interesting to see that to go from a simple, fixed nuclei (FN) treatment, where only the classical geometries of the isolated molecule and of the complex are taken into consideration, to a more realistic physical picture where ZPE corrections are included already provides a significant modification of the PA values: The binding of the positron to the molecule becomes more stable by more than 3.0% in LiH and by about 2.5% for the RbH system. The opposite trend shown by the Born Oppenheimer energies is easily explained by the increasing separation of the potential-energy minima of the XH and e^+XH curves, the latter becoming increasingly more difficult to reach from within the subspace of nuclear geometries covered by the vibrational ground state of XH. These findings present an interesting result since they tell us that the vibrational structures of the partner molecules get distorted upon attachment of the positron and are likely to markedly modify their corresponding force constants. This result has been suggested before from dynamical calculations which approached a similar problem from the positive energy range near thresholds [7], where it was found that positron scattering from vibrationally excited CH_4 and C_2H_2 gases gives rise to resonant features due to a virtual state formation between the molecules and the impinging positron. The latter state is often referred to as a “bound” state of zero energy.

The stabilization effects caused by the vibrational energy inclusion in the PA calculations can be further assessed by examining the behavior of the computed positron affinities along the vibrational ladder of the partner molecule. We have considered, for simplicity, only a portion of the vibrational states and have not reported the actual numerical values for the higher vibrational levels close to dissociation. For such levels, in fact, the LR part of the interaction potential plays a crucial role and therefore the corresponding bound vibrational levels become very sensitive to those features of the interaction.

Furthermore, we have also omitted consideration of a process involving full vibrational relaxation of the target molecule upon complex formation. This is certainly a possible process but it requires a more extensive motion of the nuclei during the time scale of the positron attachment and therefore we expect it to happen more slowly than the electronic rearrangement which follows positron attachment. In other words, we do not consider the possible dynamics that may lead to target vibrational de-excitation but rather the sudden attachment of e^+ to an already vibrationally excited molecular partner.

The results of Table VIII are also rather unexpected in that they unequivocally indicate a marked increase of complex stabilization as the molecule increases its vibrational energy content, although we do not see from the above the preferential likelihood for each transition as guided by the corresponding size of the FC factor between the initial vibrational level of the isolated XH molecule and the final level reached in the complex e^+XH .

In particular, we see that the lightest molecular partner, the LiH target, shows a steady increase in the value of its $PA(\nu)$ with $\Delta\nu=0$ by more than 40 times from the $\nu=0$ to the $\nu=17$ vibrational levels. By the same token, the NaH hydride increases this PA value by nearly 30 times in going from $\nu=0$ to $\nu=14$. The behavior of KH and RbH is less marked because their complex structures indicate shallower PECs and therefore support fewer vibrational bound states. On the other hand, they both indicate rather substantial stabilization effects on their PA values when vibrationally excited molecular partners are considered.

Another, more pictorial way of presenting the calculations is given by Fig. 2(a) for all four systems considered here: we report in that figure the dependence on the vibrational quantum state for each alkali-metal hydride of their scaled $PA(\nu)$ values of Eq. (3). The scaling is introduced to show more clearly the different gradient values exhibited along the series of molecules, and is obtained by dividing each set of $PA(\nu)$ values for the corresponding ground-state value, i.e., for the $PA(\nu=0)$ values of Table VII. The Born-Oppenheimer-type quantities are also shown in Fig. 2(b) for comparison. There is a grouping trend between the Li and Na curves on one side, and K and Rb curves on the other side. A similar trend is also seen in the behavior of dipole moments averaged over vibrational numbers ν , which are given in Fig. 3.

One clearly sees from Fig. 2(a) that the stabilization effects behave linearly for low ν values while they acquire a quadratic dependence for the larger vibrational quantum states of LiH and NaH. The linear coefficients also increase

TABLE VIII. Energetic stabilization of $PA(\nu)$ positron affinities $PA(\nu)$ as a function of the vibrational state of the partner molecule, defined as $PA(\nu) - PA(R_{eq})$. The analogous quantity is also shown for PA_{BO} . All values in eV.

ν	Stabilization $\Delta\nu=0$ PA				Stabilization of PA_{BO}			
	LiH	NaH	KH	RbH	LiH	NaH	KH	RbH
0	0.026	0.030	0.031	0.039	-0.029	-0.077	-0.094	-0.153
1	0.074	0.090	0.097	0.117	0.012	-0.028	-0.056	-0.111
2	0.121	0.152	0.163	0.193	0.054	0.019	-0.012	-0.063
3	0.179	0.216	0.234	0.271	0.097	0.067	0.033	-0.014
4	0.236	0.280	0.306	0.348	0.141	0.116	0.078	0.036
5	0.296	0.346	0.381	0.428	0.186	0.165	0.124	0.086
6	0.359	0.412	0.458	0.509	0.231	0.215	0.171	0.137
7	0.422	0.478	0.538	0.593	0.278	0.266	0.217	0.188
8	0.487	0.544	0.621	0.680	0.326	0.317	0.264	0.239
9	0.553	0.611	0.707		0.375	0.370	0.312	0.290
10	0.620	0.677			0.425	0.423	0.360	0.341
11	0.689	0.743			0.477	0.478	0.408	0.392
12	0.758	0.812			0.531	0.535	0.457	0.444
13	0.829	0.882			0.587	0.593	0.507	0.496
14	0.900	0.952			0.646	0.655	0.557	0.548
15	0.972				0.708	0.721	0.609	0.601
16	1.043				0.771	0.793	0.663	0.654
17	1.113				0.833	0.873	0.719	0.709

along the series of molecules and we can obtain from them an average gradient along each series, i.e., the average stabilization increment when the molecules increase their vibrational quantum numbers by one unit. The values of such unit increments are reported in Table IX for the present series of alkali-metal hydrides.

It is interesting to note that the values in Table IX increase along the series, as expected, and further are rather close to twice the stabilization values induced by the inclusion of the ZPE correction given in Table VI. This means that the vibrational structures are close to being harmonic, at least qualitatively, and therefore the above gradients of the ν dependence mainly describe the effects of the almost harmonic oscillator energy ladders in the partner molecules. Predomi-

nantly harmonic behavior can also be seen in the stabilization series of Born-Oppenheimer-type positron affinities of Table VIII. Finally, let us note that the electronic and positronic densities averaged over the vibrational of alkali-metal hydride molecules are quite stable for the lowest vibrational levels and can be well approximated by the quantities at equilibrium geometry. Figure 4 demonstrates this finding in the case of LiH where one sees rather dramatically the complementary locations of electron and positron densities over the molecular nuclear regions.

IV. PRESENT CONCLUSIONS

In this work we have analyzed in some detail the possible effects of the nuclear motion (vibrational dynamics) on the

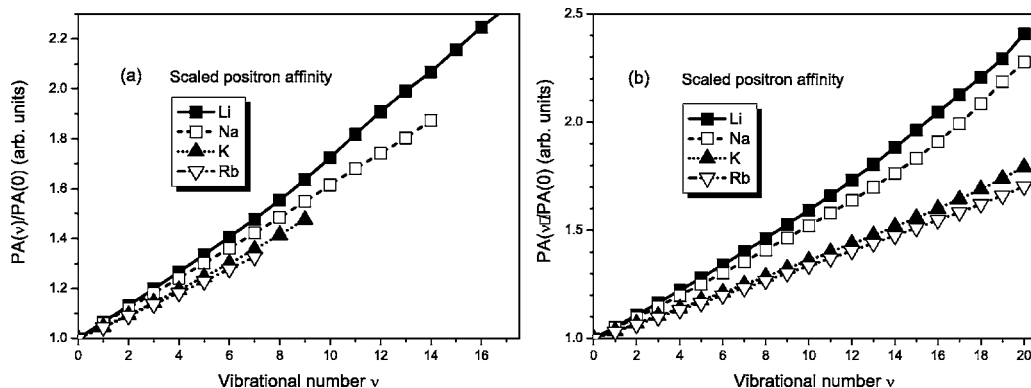


FIG. 2. Scaled positron affinities (PAs) calculated for different alkali-metal hydrides as a function of the vibrational level: (a) $\Delta\nu = 0$ PAs, (b) PA_{BO} S.

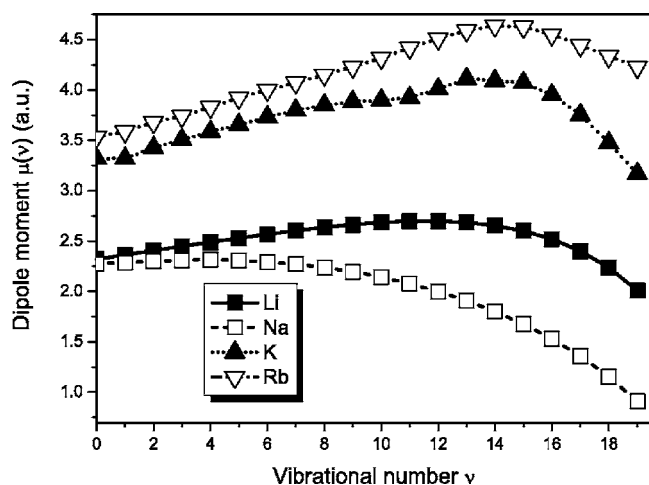


FIG. 3. Dipole moments averaged over vibration levels for different alkali-metal hydrides XH , with $X=Li, Na, K,$ and Rb .

molecular mechanism of positron attachment to simple diatomics such as the alkali-metal hydrides. We have carried out electronic bound state calculations at the MRD-CI levels, described in detail in the work of Ref. [10], for both the isolated molecules and the complexes with a positron bound to each molecule. From those calculations we have further generated the corresponding ground-state PECs, for both species and out to very large distances close to dissociation. All calculations have been further extended into the highly repulsive PEC regions of the short internuclear distance, as described in Sec. II. As also described earlier in Ref. [10], the diabatic dissociation of the more stable XH electronic state leads to $X+H$ asymptotic partners, while the positronic complex follows ionic dissociation with Ps formation on the H^- fragment: X^++HPs . This is an important feature that explains the corresponding differences between PECs in the location of their energy minima, the R_{eq} geometries of Table I, and the differences between spacings among vibrational bound states within each PEC for $J=0$, as we further discuss in Sec. III.

The calculations of ZPE corrections clearly indicate a marked stabilization effect on the PA values with respect to those obtained from FN calculations at equilibrium geometries. This is the first of our present results which helps to provide us with a better understanding of the molecular positron-attachment mechanism: the bond dilution effects occurring upon Ps formation at the H^- side of the molecule and the “through-bond” polarization effects towards the X^+ frag-

TABLE IX. Computed average stabilization value per unit of vibrational quantum number increase along the series of alkali-metal hydrides.

Molecule	$\Delta PA_{av}/meV$
LiH	64
NaH	66
KH	74
RbH	80

ment as the bonds stretch [14] help to modify, in qualitative terms, the force constants of the diatomic upon e^+ attachment and therefore cause marked differences between the vibrational ladders of XH and of e^+XH .

Such an effect is also seen from our calculations to be strongly dependent upon the vibrational quantum state of the molecular partner: this is, therefore, the second result from the present study, where we have shown that there is a strong stabilizing effect of the ($\Delta\nu=0$) PA values when the partner molecule is taken to be vibrationally excited and that such stabilizing effects increase along the series from LiH to RbH. This result is in keeping with our recent scattering calculations of simple hydrocarbons (C_2H_2 , C_2H_4 , and C_2H_6) [15], where we have shown that marked bond deformations are directly causing transient bound state formation and can enhance annihilation efficiency in such gases.

The present calculations, therefore, suggest that the vibrational content of the partner molecule, even in the case of simple diatomics, has a very strong effect on the PA value exhibited by the molecular gas and that one could achieve very marked stabilization effects if the ambient gas is “prepared” as a vibrationally excited partner during the positron-attachment experiment. Given the fact that no direct experimental evidence exists as yet for positron binding to a molecular partner, it is of interest to see from our present computational experiment that such a process could be made more likely to occur if the ambient gas were to be also vibrationally “hot.” Such an effect is expected to be even more evident in the case of larger, polyatomic gases where a much higher density of vibrational levels means that the enhancements seen here would be more easy to achieve experimentally and could possibly provide an interesting option for positron binding detection in molecular gases. It would also be likely, in such polyatomic targets, that the final “positronated” species could partially relax to a different vibrational energy content after positron attachment.

We have also presented the series of XH dipole moments averaged over vibrational wave functions of the neutral complex. We note that all alkali-metal hydrides have an overcritical value of dipole moments and could thus support, in principle, an infinite number of bound positron states if only the charge-dipole interaction potential was considered [16]. Such a dependence is of general interest, although one should remember that the physical existence of the alternative dissociation channel (X^++PsH) is not considered by the analytic model [16], and therefore no physical infinity of states is likely to occur. It is also worth noting that the electronic and positronic densities at R_{eq} and for $\nu=0$ practically coincide, and their ν dependence is rather small for low vibrational numbers, as demonstrated in this paper: it tells us that separation of charges only starts to occur as the e^+XH complex becomes vibrationally excited, and that the charge densities computed at R_{eq} may well approximate those of the low vibrational states of the molecule.

ACKNOWLEDGMENTS

The financial support of the University of Rome Research Committee, of the CASPUR computational facilities and of

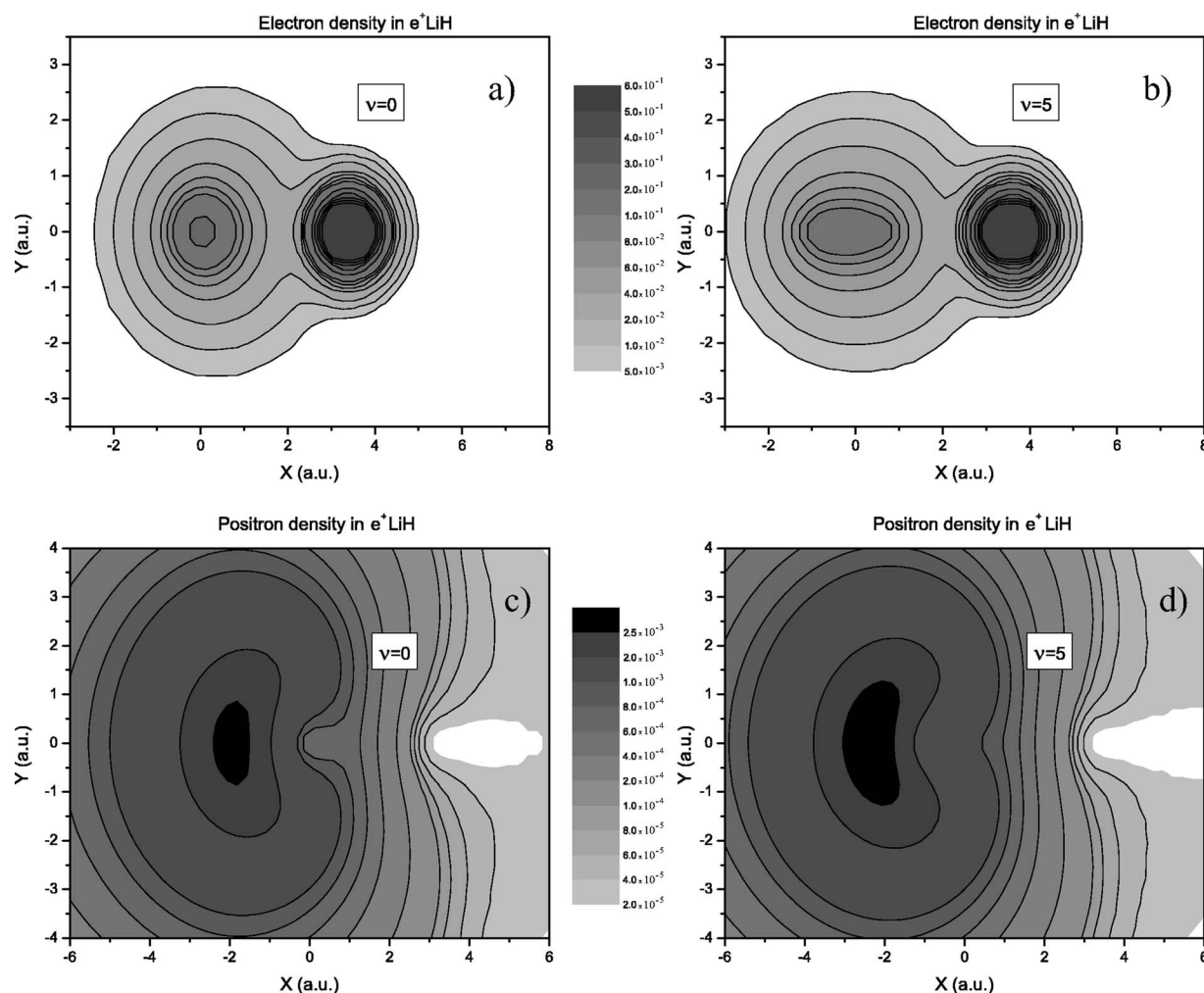


FIG. 4. Charge densities for LiH averaged over the vibrational motion of the two nuclei: (a) electron density for $\nu=0$, (b) electron density for $\nu=5$, (c) positron density for $\nu=0$, and (d) positron density for $\nu=5$.

the EU Collaborative Network Grant No. HPRN-CT-2002-00179 are gratefully acknowledged. This work was also supported by the Japan Society for the Promotion of Science, the Japanese Ministry of Science, Sports, Culture and Education (MEXT), Grant No. BU 450/14-1 of the Deutsche

Forschungsgemeinschaft, and the Fonds der Chemischen Industrie. Lukáš Pichl also acknowledges the support of the Max Planck Society, Academic Frontier Program of MEXT, and the use of the Earth Simulator supercomputer account via a JAMSTEC-based project.

- [1] C. M. Surko, G. F. Gribakin, and S. J. Buckman, *J. Phys. B* **38**, R57 (2005).
 [2] M. Kimura, O. Sueoka, A. Hamada, and Y. Itikawa, *Adv. Chem. Phys.* **111**, 537 (2000).
 [3] See e.g., H. Hotop, M.-W. Ruf, M. Allan, and I. I. Fabrikant, *Adv. At., Mol., Opt. Phys.* **49**, 85 (2003).
 [4] D. Bressanini, M. Mella, and G. Morosi, *J. Chem. Phys.* **109**, 1716 (1999).
 [5] J. Mitroy, M. W. J. Bromley, and G. G. Ryzhikh, *J. Phys. B* **35**, R81 (2002).
 [6] F. A. Gianturco, T. Mukherjee, and P. Paoletti, *Phys. Rev. A*

A56, 3638 (1997).

- [7] T. Nishimura and F. A. Gianturco, *Phys. Rev. Lett.* **90**, 183201 (2003).
 [8] M. Mella, S. Chiesa, and G. Morosi, *J. Chem. Phys.* **116**, 2852 (2002).
 [9] M. Mella, G. Morosi, D. Bressanini, and S. Elli, *J. Chem. Phys.* **113**, 6154 (2000).
 [10] R. J. Buenker, H.-P. Liebermann, V. Melnikov, M. Tachikawa, L. Pichl, and M. Kimura, *J. Phys. Chem. A* **109**, 5956 (2005).
 [11] R. J. Buenker in *“Proceedings of the Workshop on Quantum Chemistry and Molecular Physics,”* Wdlongong, Australia, ed-

- ited by R. A. Philips, [J. Mol. Struct.: THEOCHEM **123**, 291 (1985)].
- [12] R. Krebs and R. J. Buenker, J. Chem. Phys. **103**, 5613 (1995).
- [13] R. J. LeRoy, University of Waterloo, Chemical Physics Research Report No. CP-555R, 2000 (unpublished)
- [14] See; e.g., F. A. Gianturco and S. Kumar, Z. Phys. D: At., Mol. Clusters **37**, 155 (1996).
- [15] T. Nishimura and F. A. Gianturco, Phys. Rev. A **72**, 022706 (2005).
- [16] O. H. Crawford, Proc. Phys. Soc. London **91**, 279 (1967).